ADVANCES IN ATMOSPHERIC SCIENCES, VOL. 32, MARCH 2015, 301–318

A Hybrid Coupled Model for the Pacific Ocean–Atmosphere System. Part I: Description and Basic Performance

ZHANG Rong-Hua*

Key Laboratory of Ocean Circulation and Waves, Institute of Oceanology, Chinese Academy of Sciences, Qingdao 266071

(Received 15 January 2014; revised 19 May 2014; accepted 16 June 2014)

ABSTRACT

A hybrid coupled model (HCM) is constructed for El Niño–Southern Oscillation (ENSO)-related modeling studies over almost the entire Pacific basin. An ocean general circulation model is coupled to a statistical atmospheric model for interannual wind stress anomalies to represent their dominant coupling with sea surface temperatures. In addition, various relevant forcing and feedback processes exist in the region and can affect ENSO in a significant way; their effects are simply represented using historical data and are incorporated into the HCM, including stochastic forcing of atmospheric winds, and feedbacks associated with freshwater flux, ocean biology-induced heating (OBH), and tropical instability waves (TIWs). In addition to its computational efficiency, the advantages of making use of such an HCM enable these related forcing and feedback processes to be represented individually or collectively, allowing their modulating effects on ENSO to be examined in a clean and clear way. In this paper, examples are given to illustrate the ability of the HCM to depict the mean ocean state, the circulation pathways connecting the subtropics and tropics in the western Pacific, and interannual variability associated with ENSO. As satellite data are taken to parameterize processes that are not explicitly represented in the HCM, this work also demonstrates an innovative method of using remotely sensed data for climate modeling. Further model applications related with ENSO modulations by extratropical influences and by various forcings and feedbacks will be presented in Part II of this study.

Key words: hybrid coupled model, ocean–atmosphere coupling, ENSO, forcing, feedback, satellite data

Citation: Zhang, R.-H., 2015: A hybrid coupled model for the Pacific ocean–atmosphere system. Part I: Description and basic performance. *Adv. Atmos. Sci.*, **32**(3), 301–318, doi: 10.1007/s00376-014-3266-5.

1. Introduction

The coupled ocean–atmosphere system in the Pacific plays a very important role in global climate variability and change. The ENSO is the largest interannual signal originating from the ocean–atmosphere coupling within the tropical Pacific (e.g., Bjerknes, 1969; Zebiak and Cane, 1987), which affects weather and climate worldwide. In the subtropical and midlatitude regions, the subtropical gyre and the Kuroshio system are the important ocean circulation systems that directly affect regional and basin-scale climate variability over the Northern Hemisphere. Additionally, the tropics and extratropics exhibit clear interactions over the Pacific sector, which give rise to ENSO variability and the existence of low-frequency climate modes, including the Pacific decadal oscillation (PDO).

While great progress has been made in understanding the coupled ocean–atmosphere system over the Pacific, the mechanisms involved in the modulations of ENSO remain poorly understood. For example, as has been demonstrated (Gu and Philander, 1997; Kleeman et al., 1999), ENSO can be modulated by extratropical processes through the changes in the subtropical cell of the ocean (e.g., McCreary and Lu, 1994); an interactively coupled loop has been identified that involves interactions between the atmosphere and ocean, and between the tropics and extratropics over the Pacific basin (e.g., Zhang et al., 1998; Fedorov and Philander, 2000; Wang and An, 2001). In addition, ENSO can also be modulated by a variety of forcing and feedback processes in the region, including stochastic forcing (SF) of wind, freshwater flux (FWF), ocean biology-induced heating (OBH), tropical instability waves (TIWs), and so on. As all these effects are intermingled with one another, it is difficult to understand how ENSO is affected by these processes individually and collectively.

Numerical models are powerful tools to describe and understand these processes and their complicated interplay involving different dynamical regimes. In the past, various coupled atmosphere–ocean models with varying levels of complexity have been developed and can be used to investigate the interactions between the tropics and subtropics, and between different forcing and feedback processes. For example, fully coupled general circulation models (CGCMs) are avail-

* Corresponding Author: ZHANG Rong-Hua
Email: rzhang@qdio.ac.cn

able for use to represent the interplay between processes affecting the properties of ENSO. However, CGCMs are highly complex and complicated tools, with all components being interactively related with each other, making it difficult to reveal the effects of a specific process on ENSO. Additionally, fully coupled GCMs are computationally very expensive to run.

Here, we introduce a hybrid coupled model (HCM) developed for ENSO-related modeling studies, in which an ocean general circulation model (OGCM) is coupled with a simple atmospheric model for interannual wind stress (τ) variability derived from a singular value decomposition (SVD) analysis. The OGCM used in this work is the Gent–Cane OGCM (Gent and Cane, 1989), a layer model with an explicitly embedded bulk mixed layer model. As an effort to extend our previous tropics-only coupled ocean–atmosphere model (Zhang et al., 2006), the HCM developed in this work covers almost the entire Pacific basin, allowing for representations of ocean processes in the tropics and subtropics, and their interactions.

There are clear advantages of developing such an HCM for ENSO-related modeling studies. As a dominant interannual signal in the region, ENSO produces SST anomalies, which induce atmospheric wind responses that are quick and almost simultaneous in the tropical Pacific, leading to coherent relationships between interannual variations in SST and winds during ENSO cycles. Therefore, their statistical relationship from historical data can be used to construct a feedback model to simply capture wind anomalies as a response to SST variability. Therefore, such an HCM can offer an extremely efficient modeling tool for the ocean–atmosphere system in the Pacific, allowing a large number of experiments to be performed feasibly and affordably. Yet, as will be demonstrated in this paper in this paper, the HCM constructed over the Pacific basin can depict reasonably well the coupled ocean–atmosphere interactions, and in particular can give rise to a realistic simulation of interannual variability associated with ENSO. As the model covers almost the entire Pacific domain, extratropical processes and their interactions with the tropics are naturally represented in the ocean and atmosphere. Hence, the HCM can be adopted to investigate modulations of ENSO that arise from extratropical effects, which are not possible in tropics-only HCMs (e.g., Zhang et al., 2006).

In additional to extratropical processes that can exert an influence on ENSO, a variety of forcing and feedback processes exist in the Pacific. For example, ENSO also acts to produce large and coherent interannual anomalies of FWF and OBH, which can feed back onto ENSO (e.g., Zhang and Busalacchi, 2009a; Zhang et al., 2009, 2012). Similar to the treatment of winds, interannual variability of FWF and OBH can be represented as a response to ENSO-related SST anomalies; their corresponding feedback models can also be constructed from historical data and incorporated into the HCM. In particular, various parameterization schemes previously developed in our tropical model can be directly applied to the Pacific-domain model. For instance, although an ocean biology component is not explicitly included in the ocean physical system of the model, its interannual feedback effect on ENSO can still be represented using an empirical parameterization scheme constructed from satellite ocean color data (Zhang et al., 2011). Also, TIW processes have been demonstrated to be important to the heat budget and SST in the eastern tropical Pacific, but their effects are still missing in coarse-resolution climate models. At present, high-resolution satellite data are available and can be used to depict TIW-induced wind feedback (Zhang and Busalacchi, 2008, 2009b); an empirical model constructed from daily satellite data of SST and wind can be adopted and incorporated into the HCM to represent TIW-induced wind effects. Another important factor that has been demonstrated to be able to significantly modulate ENSO is SF of atmospheric winds (Kirtman and Schopf, 1998), which is missing in the HCM. Hence, a simple model has also been constructed to represent this wind forcing component (Zhang et al., 2008) and incorporated into the HCM to represent its effect on ENSO.

Taking all these together into an HCM framework, we offer a computationally efficient modeling tool that can be used to represent and understand the coupled ocean–atmosphere system for almost the entire Pacific basin, including the interactions between the subtropics and tropics. Several processes important to ENSO modulations are taken into account individually and collectively. Additionally, satellite data are used to represent feedback effects for climate modeling. For instance, a novel method is demonstrated for using satellite ocean color data to parameterize OBH in a physical ocean model, and how high-resolution satellite data can be used to represent TIW-scale wind feedback within a large-scale modeling context. Various applications are expected using this modeling framework. In this paper, examples are given to illustrate the ability of the HCM to depict the mean ocean state and interannual variability associated with ENSO. Further applications related to ENSO modulations by various forcings and feedbacks will be presented in Part II of this study.

The remainder of the paper is organized as follows. Section 2 describes the models and some observational data used. The performance of the HCM is examined using its 50-year simulation for mean climatological oceanic fields in section 3, and for interannual variability in section 4. Concluding remarks are given in section 5.

2. Data and models

Based on our previous modeling efforts within the tropical Pacific, an HCM is constructed over almost the entire Pacific domain to represent the coupled ocean–atmosphere system. Figure 1 is a schematic diagram of the HCM, which consists of an OGCM and a simplified representation of the atmosphere (including three forcing fields to the ocean: wind stress (τ), freshwater flux, and heat flux). The total wind stress (τ) can be written as $\tau = \tau_{\text{clim}} + \tau_{\text{inter}} + \tau_{\text{TIW}} + \tau_{\text{SF}}$, where τ_{clim} is the climatological part, τ_{inter} is the interannual part, τ_{SF} is the stochastic forcing part, and τ_{TIW} is the TIW

part; τ_{clim} is prescribed from observations and other wind components are parameterized in a statistical way (see details below).

The total FWF, represented by precipitation (P) minus evaporation (E), $(P–E)$, is also separated into its climatological part $[(P–E)_{clim}]$ and interannual anomaly part (FWF_{inter}), written as $FWF = (P–E)_{clim} + FWF_{inter} = (P–E)_{clim} + (P–E)_{inter}$; the climatological field, $(P–E)_{clim}$, is prescribed in the FWF calculation. The heat flux (HF) is interactively determined using an advective atmospheric mixed layer (AML) model (Seager et al., 1995); various climatological fields are specified in the heat flux calculation (Seager et al., 1995).

Furthermore, some related forcing and feedback processes are also included in the HCM to account for their effects on ENSO. For example, ocean biology-induced heating (OBH) is included in the physical ocean model; its effect on the penetrative radiation is simply represented by the attenuation depth of solar radiation in the upper ocean (H_p). Similarly, the total H_p field is separated into its climatological part $(\overline{H_p})$ and interannual anomaly part (H'_p), written as $H_p = \overline{H_p} + H'_p$. The $\overline{H_p}$ part is derived from remotely sensed ocean color data, and H'_p is estimated using its empirical model representing a response to change in the physical system. In this simplified hybrid coupled modeling system, climatological fields (τ_{clim}, SST_{clim}, $(P–E)_{clim}$, and $\overline{H_p}$) are all prescribed as seasonally varying from observations; interannual anomaly fields (τ_{inter}, $(P–E)_{inter}$ and H'_p) are diagnostically determined from their corresponding empirical submodels relating to interannual SST variability. Additionally, τ_{TIW} is estimated using its empirical model constructed from high-resolution satellite data; τ_{SF} is estimated empirically as well. All these are briefly described in this section below.

2.1. *Datasets*

Various observational and model-based data are used to construct empirical models for perturbation fields (τ_{inter}, $(P–E)_{inter}$ and H'_p), as well as to validate model simulations. Long-term climatological fields are prescribed in the HCM, including monthly-mean wind stresses (τ_{clim}) from the National Centers for Environmental Prediction–National Center for Atmospheric Research (NCEP–NCAR) reanalysis (Kalnay et al., 1996), precipitation from Xie and Arkin (1995), solar radiation from the Earth Radiation Budget

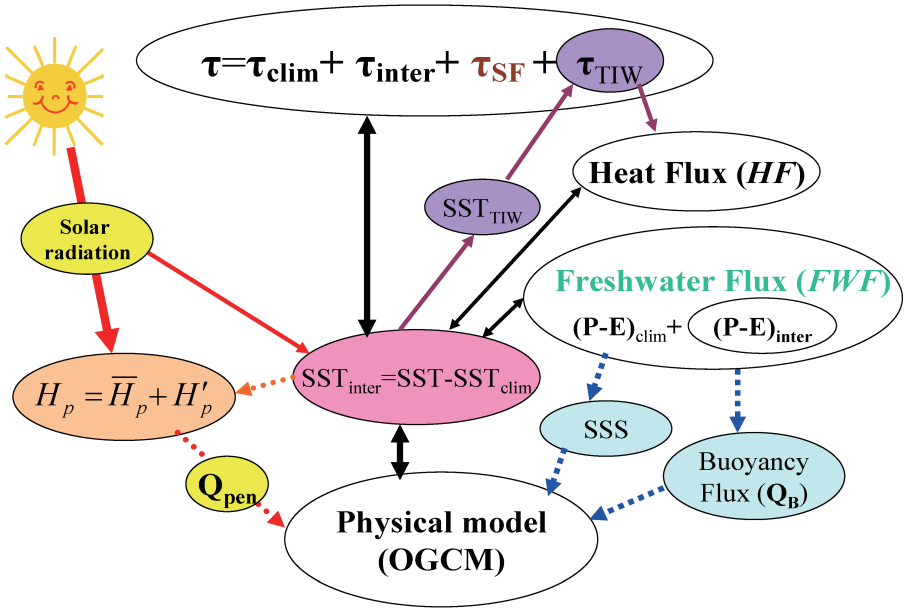

Fig. 1. Schematic diagram illustrating the hybrid coupled model (HCM), consisting of an OGCM and a simplified representation of the atmosphere, whose three forcing fields of the ocean include wind stress (τ), freshwater flux (FWF) and heat flux (HF). The total wind stress (τ) is separated into its climatological part (τ_{clim}), interannual anomaly part (τ_{inter}), stochastic forcing part (τ_{SF}), and tropical instability wave (TIW) part (τ_{TIW}), written as $\tau = \tau_{clim} + \tau_{inter} + \tau_{SF} + \tau_{TIW}$. The total FWF, represented by precipitation minus evaporation, $P–E$, is also separated into its climatological part $[(P–E)_{clim}]$ and its interannual anomaly part [FWF_{inter} or $(P–E)_{inter}$], written as $FWF = (P–E)_{clim} + (P–E)_{inter}$, which acts to have direct effects on sea surface salinity (SSS) and buoyancy flux (Q_B). The HF is calculated using an advective atmospheric mixed layer (AML) model developed by Seager et al. (1995). In addition, the ocean–atmosphere system is affected by ocean biology-induced heating (OBH), whose effects on ocean physics are simply represented by the attenuation depth of solar radiation in the upper ocean (H_p); similarly, the total H_p field is separated into its climatological part $(\overline{H_p})$ and interannual anomaly part (H'_p), written as $H_p = \overline{H_p} + H'_p$, which acts to affect the penetrative solar radiation flux out of the base of the mixed layer (Q_{pen}).

Experiment (ERBE), and cloudiness from the International Satellite Cloud Climatology Project (ISCCP). $\overline{H_p}$ is estimated using multi-year climatological ocean color data averaged over the period of September 1997 to April 2007 (McClain et al., 1998).

Interannual anomaly fields used to construct empirical models include those of observed SST from Reynolds et al. (2002), and wind stress and *P–E* obtained from an ensemble mean of a 24-member ECHAM 4.5[a] AGCM (Roeckner et al., 1996) simulation over the period 1950–99, which is forced by observed SST fields. Using the ensemble mean data for wind stress and *P–E* represents an attempt to enhance SST-forced signals by reducing atmospheric noise.

In addition, satellite data are used to represent various specific processes that are important to ENSO. For example, chlorophyll (Chl) in the ocean can affect the penetration of solar radiation in the upper ocean, but it is difficult to obtain basin-wide in situ measurements. Today, ocean color data are available from satellites and can be used to depict its interannual variability associated with ocean biology. As in our previous modeling studies (Zhang et al., 2009, 2011), this feedback is parameterized using remotely sensed ocean color data (McClain et al., 1998). Also, high-resolution satellite wind vector data are available and can be used to represent TIW-scale wind feedback (Zhang and Busalacchi, 2008, 2009b). Daily SST fields are from the Tropical Rainfall Measuring Mission (TRMM) satellite's microwave imager (TMI; Wentz et al., 2000), and surface winds are from QuikSCAT during the period 2000–07.

2.2. *Hybrid coupled ocean–atmosphere model*

As classified to be an HCM (Fig. 1), our model's ocean component is a comprehensive OGCM, while the interannual wind component is a simple statistical model. This is based on the fact that ENSO is a dominant driving force of the coupled ocean–atmosphere system in the Pacific, acting to produce large-scale interannual SST anomalies, which in turn induce quick surface wind responses. The coherent relationships between interannual variations in SSTs and winds are used to construct an empirical model. Additionally, some related feedback processes are incorporated in the HCM to represent their possible effects on ENSO.

2.2.1. *OGCM*

The ocean model used is based on the primitive equation model with the reduced gravity approximation developed by Gent and Cane (1989). In the vertical direction, the ocean model includes a mixed layer and a number of layers below specified on a sigma coordinate (thus referred to as a layer model). The depth of the mixed layer (top layer) and thickness of the last sigma layer (bottom layer) are determined prognostically, while the thickness of the remaining layers are calculated in such a way that the ratio of each sigma layer to the total depth is held to its prescribed value. In addition, several related efforts made in the past have improved this ocean model significantly. For example, a hybrid vertical mixing scheme was developed and embedded into the ocean model (Chen et al., 1994); the OGCM is coupled to an advective AML model to estimate sea surface heat fluxes (Murtugudde et al., 1996); and salinity effects have been included in the model with freshwater flux treated as a natural boundary condition (Murtugudde and Busalacchi, 1998). Also, the effects of penetrative radiation in the upper ocean have been taken into account; remotely sensed ocean color data are adopted to prescribe seasonally varying climatological attenuation depths (Murtugudde et al., 2002; Ballabrera-Poy et al., 2007).

The OGCM covers the Pacific domain from 40°S to 60°N and from 124°E to 76°W; its zonal resolution is uniform (1°), and its meridional resolution is stretched in latitude [0.31° within 5°S–5°N, 0.5° in the off-equatorial (5°–15°) regions, and 1° poleward of 30°]. In the vertical direction, the OGCM has 31 layers, with the first layer treated as a bulk mixed layer. Sponge layers are introduced near the OGCM southern boundaries (poleward of 35°S); that is, a Newtonian term is included in the temperature and salinity equations, acting to relax the model temperature and salinity fields to observational data specified using the World Database (Levitus et al., 2005). The OGCM is initiated from the Levitus temperature and salinity fields and is integrated for more than 50 years using prescribed atmospheric climatological forcing fields (OGCM spinup), including wind stress from the NCEP–NCAR reanalysis products averaged over the period 1950–2000. Note that a 50-year ocean spinup is quite short and may be insufficient to achieve a quasiequilibrium state for starting climate simulations. However, the model used is a reduced gravity model designed to describe ocean circulation in the upper ocean (upper 2000 m or so); the shortness of the OGCM spinup period does not matter for the purpose of this specific research (i.e., ENSO simulation).

2.2.2. *Empirical model for interannual wind stress variability*

The atmospheric τ model adopted in this work is a statistical one, specifically relating its interannual variability to SST anomalies, written as $\tau_{\text{inter}} = \alpha_{\text{inter}} F_{\text{inter}}(\text{SST}_{\text{inter}})$, where $\text{SST}_{\text{inter}}$ represents interannual SST anomalies, F_{inter} represents the relationships between interannual variations in τ and SST, and α_{inter} is a scalar parameter introduced to represent the strength of interannual wind forcing of the ocean.

The F_{inter} function is estimated using an SVD analysis of the covariance matrix that is calculated from time series of monthly-mean $\text{SST}_{\text{inter}}$ and τ_{inter} fields (e.g., Barnett et al., 1993; Chang et al., 2001). In this work, a combined SVD analysis is performed based on the covariance among anomalies of SST, zonal and meridional wind stress components (Zhang et al., 2003, 2006). Due to computational limitations, the SVD analysis is performed on a horizontal resolution of 2° zonally, and stretched spacing meridionally from 0.5° within 10° of the equator to 3° poleward (note

[a]The ECHAM4.5 AGCM is a model developed by the Max Planck Institute for Meteorology (MPI) and the European Center for Medium-Range Weather Forecasts; see details in Roeckner et al. (1996).

that the horizontal resolution for SST_{inter} and τ_{inter} analyses is different from that of the OGCM). In time, the SVD analysis is performed using historical SST_{inter} and τ_{inter} data over the 1963–96 period (34 years). With these specifications, the dimensions of the matrix for the SVD analyses are $83 \times 128 \times 408$ (zonal and meridional grid points over the entire Pacific ocean, and 34-year temporal sampling from 1963 to 1996).

Figure 2 illustrates the spatial patterns of the first SVD mode derived for SST and wind stress in the Pacific basin. Here, the SVD analysis is performed on all time series data during 1963–96 (i.e., irrespective of seasons) to obtain singular vectors, singular values, and the corresponding time coefficients. The first five singular values are about 239, 55, 32, 21 and 16, with the squared covariance fraction being about 91%, 5%, 2%, 1% and 0.4%, respectively.

The temporal expansion coefficients (figures not shown) clearly indicate that the first mode describes interannual variability associated with ENSO events. The corresponding spatial patterns of SST and wind (Figs. 2a and b) indicate that their large amplitude is located in the tropical Pacific; the primary coupled mode is composed of a wind variability center over the western-central Pacific that covaries with anomalous SST in the eastern and central equatorial Pacific. For example, during El Niño, large warm SST anomalies in the eastern equatorial Pacific (Fig. 2a) are accompanied by westerly wind anomalies over the central equatorial Pacific around the date line (Fig. 2b). The second mode (figures not shown) also shows a coherent relationship between these fields, with the spatial patterns representing transition stages of ENSO evolution. Note that the second SVD mode has its largest amplitude located in the extratropics.

Based on this SVD analysis, an empirical τ_{inter} model can be constructed to relate interannual variations in wind stress

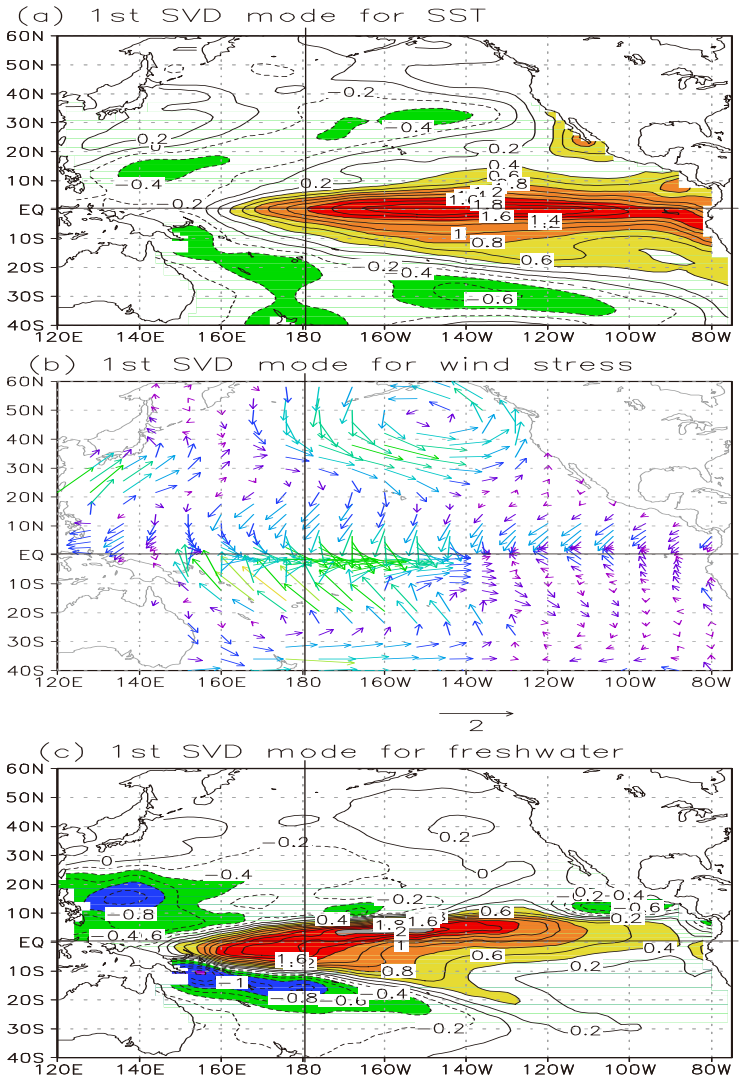

Fig. 2. The spatial patterns of the first SVD mode derived for (a) SST, (b) wind stress (vectors), and (c) *P–E*. The SVD analyses are performed during the period 1963–96. The contour interval is 0.2 in (a) and (c); the arrow in (b) indicates 2 dyn cm^{-2} (1 dyn $= 10^{-5}$ N) for the τ magnitude.

to those in SST, representing a dominant wind–SST coupling in the Pacific. As demonstrated by Barnett et al. (1993), interannual wind responses to a given SST anomaly are sensitively dependent on seasons during ENSO evolution. This seasonality needs to be taken into account when constructing the τ_{inter} model. To this end, the SVD analyses are performed separately for each calendar month, thus yielding 12 seasonally varying sub-models (e.g., Zhang and Zebiak, 2002; Zhang and Busalacchi, 2005). Thus, given an SST anomaly, the interannual wind response can be calculated according to the constructed τ_{inter} model. In the consideration of the sequence of the singular values (figure not shown) and the reconstruction testing of the τ_{inter} fields from SST anomalies, the first five leading SVD modes are retained in the empirical τ_{inter} model for having its reasonable amplitude.

2.3. *Representing forcing and feedback processes in the HCM*

While interannual wind forcing is a major factor determining ENSO dynamics, other forcing and feedback processes also exist in the Pacific and can modulate ENSO in a substantial way (Fig. 1), including FWF, OBH, and TIW-scale wind feedback. Additionally, wind forcing is stochastic in nature; as demonstrated by previous studies, SF of atmospheric winds can affect ENSO in a significant way (Kirtman and Schopf, 1998; Zhang et al., 2008). In our previous tropical Pacific modeling studies, statistical modeling tools were developed to represent these forcings and feedbacks; in this study, they are directly applied to the Pacific HCM, as described below.

2.3.1. *Stochastic forcing model for wind stress*

Wind stress anomalies that force the ocean model consist of an interannually varying signal part and a noise part. The former is estimated using the SVD-based empirical τ_{inter} model (see section 2.2.2) as a response to interannual SST variations (i.e., an SST forced signal). The latter (the SF part) is of stochastic nature (i.e., not explicitly related with an external forcing). This SF wind forcing part has been demonstrated to have significant effects on ENSO (e.g., Zhang et al., 2008), and thus needs to be represented in the HCM. Details of the construction of the SF wind part can be found in Zhang et al. (2008) and will be presented in Part II of this study.

2.3.2. *Freshwater flux forcing: precipitation minus evaporation*

Observational and modeling studies indicate that the interannual variability of *P–E* and SST are coherently related with each other over the tropical Pacific, with a dominant SST control of *P–E*. In particular, interannual variations in *P–E* closely follow those in SST during ENSO evolution. This provides a physical basis for constructing a statistical feedback model for interannual FWF responses to interannual SST anomalies.

To depict statistically optimized empirical modes of their co-variability, an SVD technique is also adopted for interannual anomaly fields of observed SST and *P–E* estimated from the ECHAM4.5 AGCM ensemble simulations. First, monthly-mean data are normalized in terms of their spatially averaged standard deviation to form the covariance matrix. Then, an SVD analysis is conducted on all time series data irrespective of season over the 1963–96 period (a total of 34 years of data). The first five singular values are about 3023, 712, 429, 343 and 242, with squared covariance fractions of about 89%, 5%, 2%, 1% and 0.6%, respectively.

Figure 2c shows the spatial patterns of the first SVD mode for FWF. The corresponding temporal expansion coefficients (figures not shown) indicate that the first mode describes interannual FWF variability associated with ENSO events. The spatial pattern (Fig. 2c) illustrates that the primary coupled mode of the variability is composed of a large FWF anomaly center in the central equatorial Pacific that co-varies with anomalous SST in the eastern and central equatorial Pacific (Fig. 2a). The second mode (figures not shown) also shows coherent relationship between FWF and SST both in time and space.

Based on this SVD analysis, an empirical FWF model is constructed using their derived spatial eigenvectors of the SVD modes (e.g., Zhang and Busalacchi, 2009b), written as $\text{FWF}_{\text{inter}} = \alpha_{\text{FWF}} F_{\text{FWF}}(\text{SST}_{\text{inter}})$, where F_{FWF} represents the relationships between interannual variations in FWF and SST determined from the SVD analyses. The $\text{FWF}_{\text{inter}}$ model is constructed with the same period and horizontal resolution as in the τ_{inter} model; the first five leading SVD modes are retained for having reasonable amplitude in the $\text{FWF}_{\text{inter}}$ simulation. Thus, a given interannual anomaly of SST can be converted into an anomaly of FWF for use in the HCM.

It turns out that the $\text{FWF}_{\text{inter}}$ model can successfully capture large-scale interannual FWF variability associated with ENSO evolution. For instance, as shown in Fig. 2c, the spatial patterns display interannual FWF anomalies at the mature phase of ENSO events. During El Niño, a warm SST anomaly induces an increase both in *P* and *E*, but *P* increases significantly over a broad region in the central basin. As a result, El Niño is accompanied by a positive FWF anomaly over the intertropical convergence zone (ITCZ) in the central and eastern tropical Pacific (i.e., anomalous FWF into the ocean due to the dominance of *P* over *E*). During La Niña, an opposite pattern is seen, with a cold SST anomaly being accompanied by a negative FWF anomaly (i.e., a net loss of freshwater from the ocean).

2.3.3. *Tropical-instability-wave-induced wind feedback*

TIWs are intraseasonal, small-scale phenomena that are prominently seen over the central-eastern tropical Pacific. As has long been recognized (e.g., Bryden and Brady, 1989), they are an important component in the tropical Pacific climate system, having an influence on heat and momentum transport at the equator in the ocean (e.g., Kessler et al., 1998; Jochum et al., 2005). Recent high-resolution satellite data indicate that TIWs are accompanied by large wind perturbations, giving rise to a wind feedback onto the ocean and coupled air–sea interactions at TIW scales (e.g., Chel-

ton et al., 2001). Due to TIW roles in the climate system of the tropical Pacific, it is important to represent TIW-induced surface wind feedback effects on ENSO. However, this process is obviously missing in the HCM since its atmospheric component is a statistical one with a low horizontal resolution designed to capture large-scale wind stress variability. In our previous studies (Zhang and Busalacchi, 2008, 2009b), high-resolution satellite data were used to develop an empirical model for TIW-induced wind stress perturbations ($\tau_{\rm TIW}$) to capture TIW-induced small-scale processes in the large-scale HCM; in this work, this method is directly applied to the Pacific-domain HCM.

To extract TIW-scale SST and wind stress signals ($\rm SST_{TIW}$ and $\tau_{\rm TIW}$), a spatial high-pass filter is applied to their daily data (removing the slow-varying background mean fields by subtracting a 12° zonal moving average from the original data). Then, a standard SVD analysis is applied to the resultant $\rm SST_{TIW}$ and $\tau_{\rm TIW}$ fields to determine their statistically optimized empirical modes, from which an empirical model is constructed for $\tau_{\rm TIW}$, written as $\tau_{\rm TIW} = \alpha_{\rm TIW} F_{\rm TIW}(\rm SST_{TIW})$, where $F_{\rm TIW}$ represents the SVD-determined empirical relationships between $\rm SST_{TIW}$ and $\tau_{\rm TIW}$, and $\alpha_{\rm TIW}$ is a scalar parameter introduced to represent TIW wind feedback intensity. Thus, given an $\rm SST_{TIW}$ field, $\tau_{\rm TIW}$ can be determined accordingly. The SVD analysis is performed on data over the 2000–07 period and at the OGCM grid ($1^\circ \times 0.5^\circ$) in the central-eastern tropical Pacific (from 15°S to 15°N and from 180° to 76°W); see details in Zhang and Busalacchi (2009b).

Note that the $\tau_{\rm inter}$ component is determined at a coarse horizontal resolution using the $\tau_{\rm inter}$ model, and thus TIWs are not explicitly resolved in the large-scale coupled ocean–atmosphere context. Nevertheless, the $\tau_{\rm TIW}$ component can be estimated at a relatively high resolution using the $\tau_{\rm TIW}$–$\rm SST_{TIW}$ relationship. That is, this regional $\tau_{\rm TIW}$ model can be embedded into the HCM to capture the TIW wind forcing effect on the ocean, allowing for the representation of TIW-induced wind feedback on ENSO variability within a large-scale coupled ocean–atmosphere modeling context. Interactions among processes with varying spatiotemporal scales can be represented, including ocean–atmosphere couplings at TIW scales and ENSO scales.

2.3.4. *Ocean biology-induced heating effects*

In addition to physical processes, it has been demonstrated that ocean biology can modulate the heat budget in the upper ocean (Lewis et al., 1990). In particular, recent observational analyses and modeling studies have revealed significant effects of ocean biology on the mean climate and its low-frequency variability in the tropical Pacific. However, the HCM does not explicitly include a marine ecosystem component, and the related bio–climate coupling is not taken into account. Today, ocean color data from satellites are available and can be used to characterize basin-scale variability patterns of ocean biology and quantify its relationships with physical parameters. For example, the effect of ocean biology-induced heating can be simply represented by the penetration depth of solar radiation in the upper ocean ($H_{\rm p}$).

As a dominant source for ocean biology variability, ENSO induces large $H_{\rm p}$ anomalies over the tropical Pacific, whose spatiotemporal evolution exhibits a good relationship with SST. So, interannual anomalies of $H_{\rm p}$ can be treated as a response to those of SST in association with ENSO. Similar to τ and FWF, the total $H_{\rm p}$ field can be separated into its climatological part (seasonally varying) and interannual anomaly part. The former is prescribed by using multi-year ocean color data over the period of September 1997 to April 2007 (McClain et al., 1998); the latter can be determined using an empirical model to represent its interannual response to changes in SST (Zhang et al., 2011).

Similar to $\tau_{\rm inter}$ and $(P–E)_{\rm inter}$, an empirical $H_{\rm p}$ model can be constructed, written as $H'_{\rm p} = \alpha_{\rm Hp} F_{\rm Hp}$ ($\rm SST_{inter}$), in which $F_{\rm Hp}$ represents the SVD-based statistical relationships between interannual variations in $H_{\rm p}$ and SST, and $\alpha_{\rm Hp}$ is a rescaling parameter that is introduced to represent the amplitude of interannual $H_{\rm p}$ variability. As indicated in the SVD analysis performed by Zhang et al. (2011), the first five SVD modes contain about 65% of the covariance between interannual $H_{\rm p}$ and SST variations. To capture its amplitude using the SVD-based $H_{\rm p}$ model, $\alpha_{\rm Hp} = 2$ needs to be taken when the first five modes are retained (Zhang et al., 2011). Thus, given an SST anomaly, the $H_{\rm p}$ response can be determined from its empirical model. The $H_{\rm p}$ model is also embedded into the HCM to represent its penetration effects on solar radiation in the upper ocean. As such, interannual $H_{\rm p}$ anomalies are parameterized, with the related ocean biology-induced climate feedback being captured in the HCM.

2.4. *The coupled system and model experiment designs*

The coupling among these components (Fig. 1) is implemented as follows. At each time step, the OGCM calculates SST fields, whose interannual anomalies are obtained relative to its uncoupled climatology ($\rm SST_{clim}$, which is predetermined from the OGCM-only run forced by observed climatological atmospheric fields). The resultant interannual SST anomaly field is then used to calculate interannual anomalies of τ, FWF and $H_{\rm p}$ using their corresponding empirical models. These interannual anomalies are then added onto their prescribed climatological fields for use in the HCM. Also, TIW-scale wind and SF wind parts can be included in the HCM.

The OGCM is initiated from the World Ocean Atlas (WOA01) temperature and salinity fields (Levitus et al., 2005), and is integrated for more than 50 years using climatological atmospheric forcing fields. Based on this ocean spinup, the HCM is then initiated with an imposed westerly wind anomaly for eight months. Evolution of anomalous conditions thereafter is determined solely by coupled ocean–atmosphere interactions within the system. As examined previously by Barnett et al. (1993), coupled behaviors sensitively depend on the so-called relative coupling coefficient ($\alpha_{\rm inter}$); i.e., the wind stress anomalies from the $\tau_{\rm inter}$ model can be further scaled by this parameter. Several tun-

ing experiments are performed with different values of α_{inter} to examine ways the coupled interannual variability can be sustained in the HCM. It is found that taking $\alpha_{\text{inter}} = 1.3$ can produce a sustainable interannual variability in the HCM. Similarly, the other scalar parameters (α_{FWF}, α_{TIW}, and α_{Hp}) are also examined to represent the related feedbacks with a reasonable intensity; see details in Zhang et al. (2006, 2009) and Zhang and Busalacchi (2009b). In this paper, a reference run is performed using the HCM in which only large-scale $\text{SST}_{\text{inter}}$–$\tau_{\text{inter}}$ coupling and the FWF effect are taken into account, while other forcing and feedback processes are not taken into account (i. e., $\alpha_{\text{inter}} = 1.3$, $\alpha_{\text{FWF}} = 1.0$, $\alpha_{\text{SF}} = 0.0$, $\alpha_{\text{TIW}} = 0.0$, and $\alpha_{\text{Hp}} = 0.0$). The related forcing and feedback effects (i.e., SF, TIW and OBH) will be analyzed in the Part II of this study.

3. Simulated long-term climatology in the ocean

A 50-year reference run is performed to illustrate the performance of the HCM. The outputs are used to demonstrate its ability to simulate the annual mean, seasonal variations, and interannual variability. In this section, the resultant mean climatological fields are presented below.

3.1. *Annual-mean ocean state*

Figures 3 and 4 illustrate examples of some selected annual-mean fields simulated from the reference run. The horizontal distribution of annual-mean SST fields bear a strong resemble to the corresponding observed one (Fig. 3), with the warm pool in the west and the cold tongue in the east.

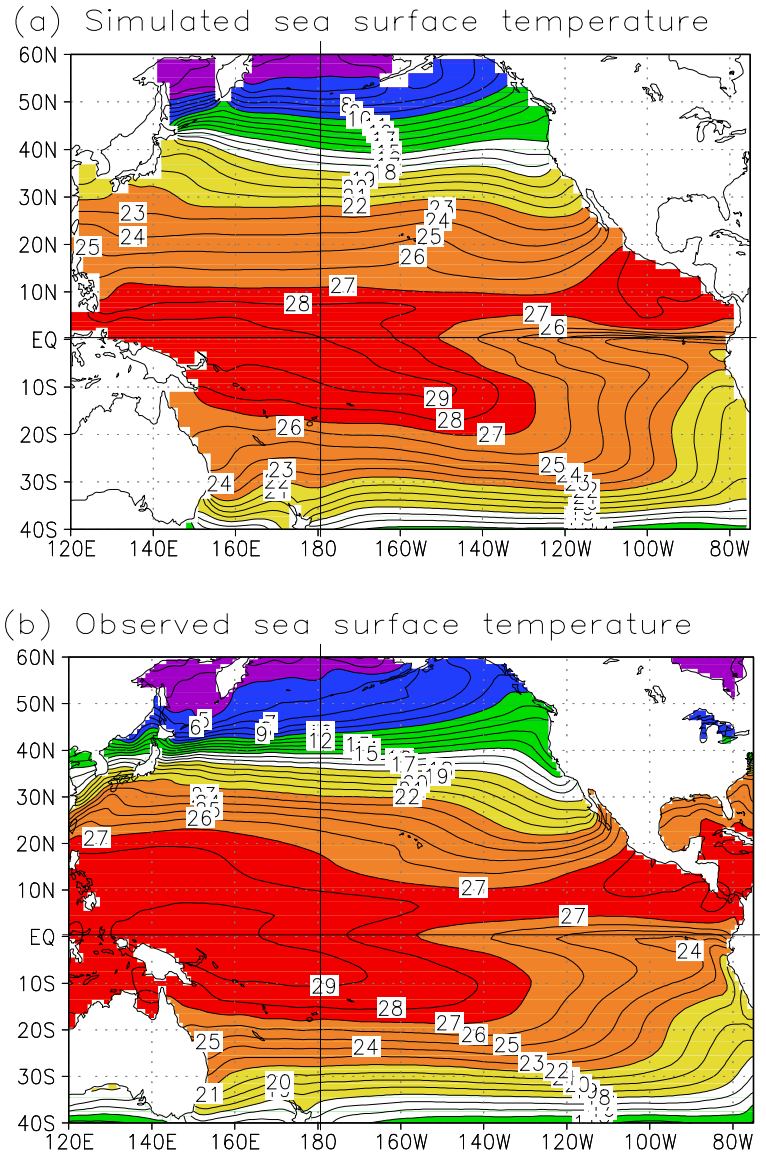

Fig. 3. Horizontal distributions of annual-mean SST fields for (a) the HCM simulation and (b) observation from NOAA Optimum Interpolation SST V2 data (climatological fields are averaged over the period 1971–2000). The contour interval is 1°C.

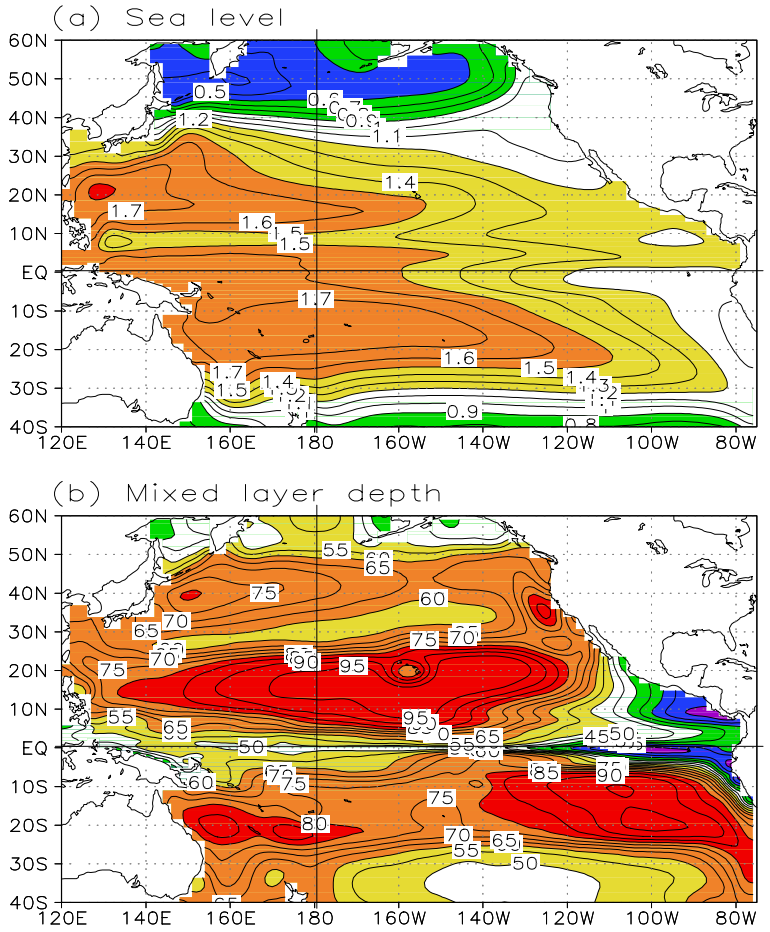

Fig. 4. Horizontal distributions of annual-mean fields simulated from the HCM for (a) sea level, and (b) mixed layer depth. The contour interval is 0.1 m in (a), and 5 m in (b).

Detailed comparisons between the HCM simulation (Fig. 3a) and observation (Fig. 3b) also reveal some discrepancies, including the simulated SST being considerably too cold in the far eastern equatorial Pacific and along the western coast of South America. The sea level (SL) exhibits well-defined trough and ridge structures in the tropical Pacific, and gyre patterns in the subtropical and subpolar regions of the North Pacific (Fig. 4a). The mixed layer depth (MLD) simulated from the HCM (Fig. 4b) is in good agreement with the corresponding observed one (e.g., Monterey and Levitus, 1997). Note that the MLD is treated as a prognostic variable in the model, which is explicitly computed using a bulk mixed-layer model (Chen et al., 1994).

More examples of vertical distributions of the simulated equatorial currents and thermal fields are displayed in Figs. 5 and 6. The HCM realistically captures the current system and temperature structure in the tropical Pacific, including the North Equatorial Current (NEC), the South Equatorial Current (SEC), the North Equatorial Countercurrent (NECC), and the Equatorial Undercurrent (EUC). Also, as seen in Fig. 6a, the HCM depicts a strong meridional boundary flow in the western North Pacific, with its maximum location along 129°E at 8°N; this boundary flow is referred to as the low-latitude western boundary current (LLWBC), which plays an important role in the water and property exchanges from the subtropics to the tropics. However, it is clear that its amplitude is underestimated significantly.

3.2. *Mean ocean circulation pathways in the western Pacific*

As has been demonstrated (e.g., McCreary and Lu, 1994; Gu and Philander, 1997; Rothstein et al., 1998), the tropical Pacific Ocean features complicated circulation pathways connecting the extratropics to the tropics, including the subtropical cells (STCs) and LLWBCs. Figure 7 illustrates the structure of mean circulation pathways in the western tropical Pacific as represented by SL and mixed-layer currents simulated from the HCM. There is a clear path that makes a connection for waters from the subtropics to the equatorial regions over the western tropical Pacific; some subtropical waters of the North Pacific flow southward through the LLWBC and eastward along the NECC, making direct routes to the equator in the interior regions (e.g., Rothstein et al., 1998; Zhang et al., 1999, 2001). Therefore, the LLWBC and NECC pathways indicate a conveyer belt of water exchange between the subtropics and tropics in the western North Pacific. At the

equator, waters in the west are transported eastward along the EUC pathway into the eastern Pacific (Figs. 5a and 6b). As the thermocline shoals along the equator from the west to the east (Fig. 5a), thermal conditions at subsurface depths in the west can directly influence SSTs in the eastern equatorial Pacific. It is conceivable that thermal conditions in the subtropical subduction regions can affect SST in the eastern equatorial Pacific through the STCs, a mechanism for connections between variations in the subtropics and tropics.

3.3. *Seasonal variation*

Figures 8 and 9 display examples of the simulated annual cycles of SST, MLD and surface zonal currents along the equator. Clearly, the simulated seasonal variation is in good agreement with corresponding observations. For example, large seasonal SST fluctuations are apparent in the eastern equatorial Pacific: a warming occurs during spring and a cooling takes place during fall (Fig. 8). Note, however, that the HCM simulation also exhibits some obvious biases compared with corresponding observations. For instance, the simulated seasonal cycle is underestimated with incorrect phase in the eastern equatorial Pacific. While the observed warming occurs in March and cooling in September, the simulated warming and cooling take place in April and August, respectively. These model biases could be related to the fact that TIWs and other forcing/feedback effects are not adequately represented in the reference HCM run; the effects involved will be examined in part II of this work.

The seasonal cycle of the MLD (Fig. 9a) is similar to the observed (e.g., Monterey and Levitus, 1997), including the shoaling in spring and deepening in fall over the eastern equatorial Pacific. One notable feature that is captured well in the HCM is the springtime reverse of the SEC in the central-eastern equatorial Pacific (Fig. 9b), which is clearly related to the seasonal SST warming (Fig. 8b). Figure 10 presents one more example of detailed vertical distributions of zonal currents and temperature fields and their seasonal variations. Some well-known features simulated well in the HCM include the seasonal variations in the EUC amplitude and its core depth (Fig. 10a), the reversal of the SEC and the surfacing of the EUC in spring (Fig. 9a), and the corresponding spring-time surface warming (Fig. 10b), respectively. The

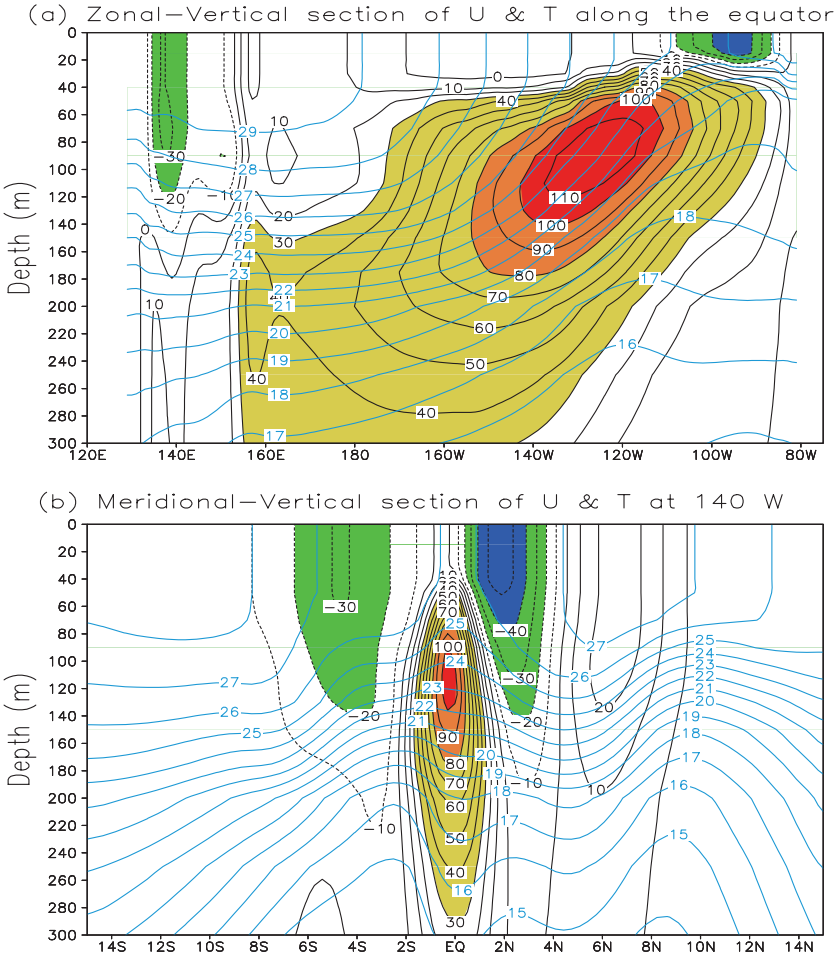

Fig. 5. Simulated annual-mean zonal currents for (a) zonal–vertical section along the equator and (b) meridional–vertical section along 140°W, with annual-mean temperature fields superimposed. The contour interval is 10 cm s^{-1} for zonal currents and 1°C for temperature.

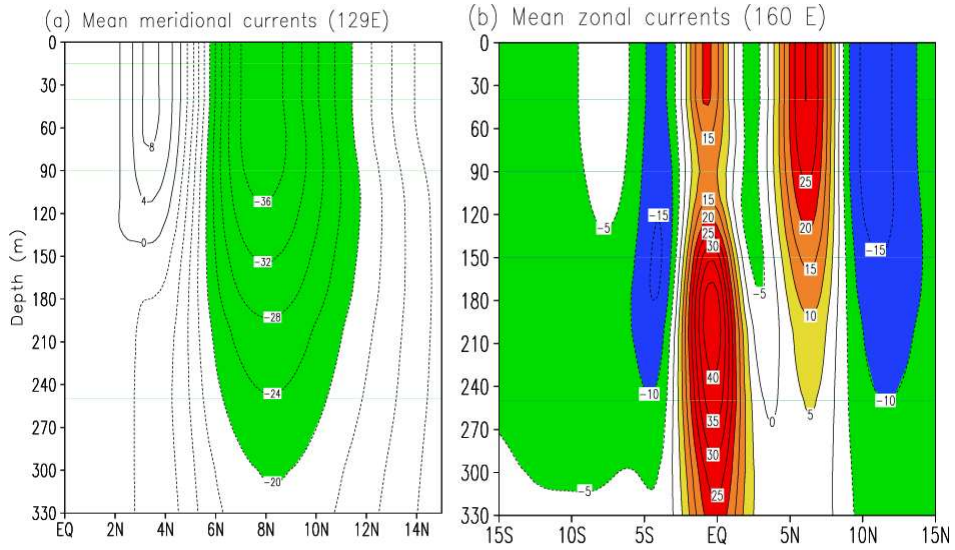

Fig. 6. Annual-mean fields simulated from the HCM for meridional–depth sections of (a) meridional velocity along 129°E and of (b) zonal velocity along 160°E. The contour interval is 4 cm s^{-1} in (a) and 5 cm s^{-1} in (b).

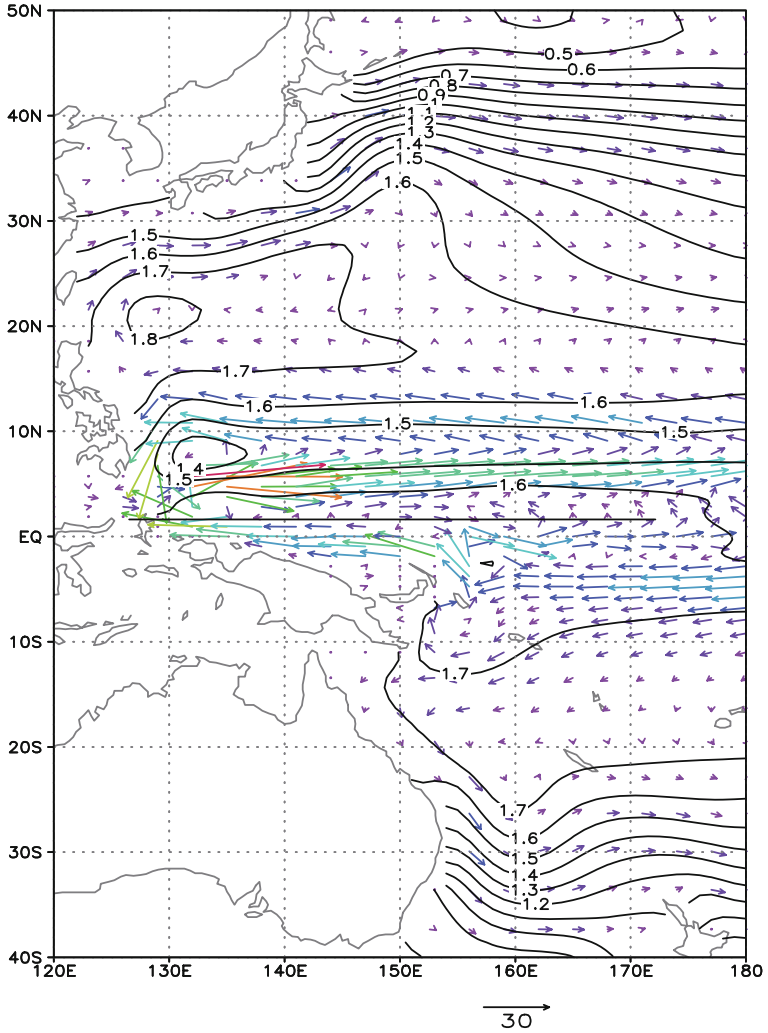

Fig. 7. Simulated annual-mean fields for sea level (contours) and mixed-layer currents (vectors) in the western Pacific. The contour interval is 0.1 m, with the given arrow (current scale) being 30 cm s^{-1}.

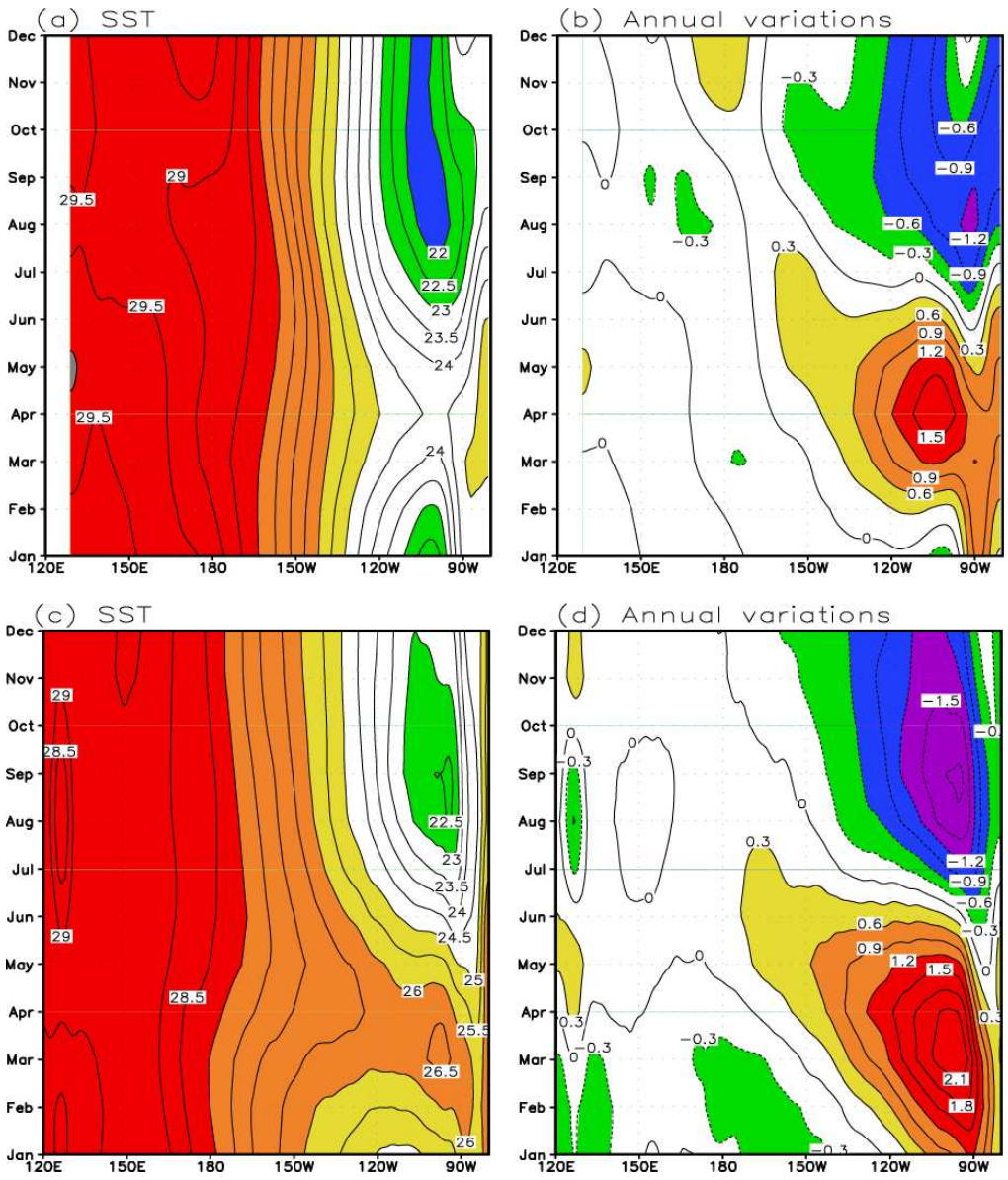

Fig. 8. SST seasonal cycle (left panels) and annual variation (relative to its annual mean; right panels) along the equator for the (a, b) HCM simulation and (c, d) observation. The contour interval is 0.5°C in (a, c) and 0.3°C in (b, d).

HCM simulation can be well compared with the corresponding observation as presented in Zhang and Zebiak (2002).

4. Simulated interannual variability

Figure 11 displays examples of interannual variability simulated from the reference run. As has been extensively studied, interannual variability in the tropical Pacific is dominated by ENSO events, which are determined by the coupling among SST, winds and the thermocline (e.g., Bjerknes, 1969). Encouragingly, the HCM can realistically capture interannual oscillations associated with El Niño and La Niña events. The overall time scales of simulated interannual variability, the spatiotemporal evolution and coherent phase relationships among various atmospheric and oceanic anomalies are consistent with observations, which have been described before (e.g., Zhang and Levitus, 1997; Zhang and Rothstein, 1998).

For example, the total SST fields (Fig. 11a) clearly display large zonal displacements of the warm pool in the west and cold tongue in the east during ENSO cycles. During El Niño, the cold tongue shrinks in the east, with warm waters in the west extending eastward along the equator (e.g., the 26°C isotherm of SST is seen to extend to east of 120°W). During La Niña, the warm pool retreats to the west, whereas the cold tongue in the east develops strongly and expands westward along the equator, with the 25°C isotherm of SST being located west of 150°W. Interannual variations in SST and sur-

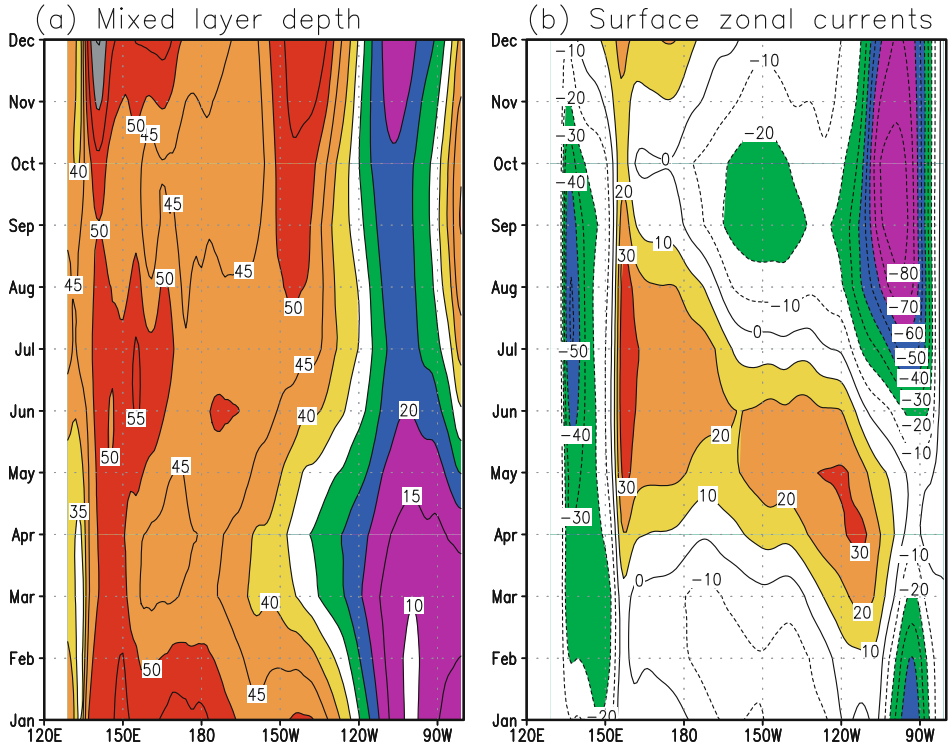

Fig. 9. Seasonal cycles along the equator for (a) MLD and (b) surface zonal currents simulated in the HCM. The contour interval is 5 m in (a) and 10 cm s^{-1} in (b).

face wind do not exhibit obvious propagation at the equator; they are almost in phase in time, with a zonal shift in space. The largest SST anomalies occur in the central and eastern equatorial Pacific (Fig. 11b), while the largest wind variability is located near the date line (Fig. 11c).

Coherent relationships between these anomaly fields can be more clearly seen in their horizontal patterns (figures not shown). During El Niño, for example, warm SST anomalies are located in the eastern equatorial Pacific, accompanied by westerly wind anomalies to the west in the tropical Pacific and a cyclonic circulation around the Aleutian Low region in the North Pacific (i.e., the Aleutian Low is intensified in response to warm SST anomalies in the tropics). During La Niña, an opposite pattern is seen, with cold SST anomalies being associated with easterly wind anomalies in the tropics and an anticyclonic circulation around the Aleutian Low region (i.e., the Aleutian Low is weakened in response to cold SST anomalies in the tropics). At the transitional stage from El Niño to La Niña, no significant anomalies are seen in the surface fields of SST and wind, but large thermal anomalies are seen at subsurface depths. The commonly adopted Niño3.4 index is used to quantify the dominant time scales of interannual variability. A wavelet analysis suggests that interannual oscillations in the HCM indicate two peaks at about 2 years and 4 years; the corresponding observation indicates a dominance of about 4.8 years. Interannual SST variability is further quantified in Fig. 12. The amplitude and structure are captured well in the tropical Pacific. For example, the standard deviations of the Niño1+2, Niño3, Niño3+4, and Niño4 SST anomalies are 0.63, 1.04, 1.22 and 0.89, respectively. Some model biases are also evident. For example, the maximum SST anomalies tend to occur around 120°W–180°E, which is too far west than observed, and the Niño1+2 SST anomalies are much weaker than observed. Also, the reference HCM simulation cannot capture the so-called eastern Pacific (EP) and central Pacific (CP) El Niño events.

5. Concluding remarks

ENSO is the largest interannual signal arising from air–sea interactions in the tropical Pacific. It has been examined extensively using tropical ocean–atmosphere models in the Pacific. Since ENSO can also be modulated by extratropical processes, it is necessary to take into account the modulating effects coming from the subtropics and midlatitudes. In this work, a hybrid coupled ocean–atmosphere model (HCM) is developed for almost the entire Pacific basin; its atmospheric component is taken to be a statistical one. Such a configuration can be justified by the fact that interannual variability in the region is dominated by ENSO, acting to generate large SST anomalies, which induce atmospheric responses that are quick and coherent at large scales. Therefore, the related surface wind variability can be treated as a feedback process, with the relationships between interannual variations in SST and surface wind being established from historical data. Ac-

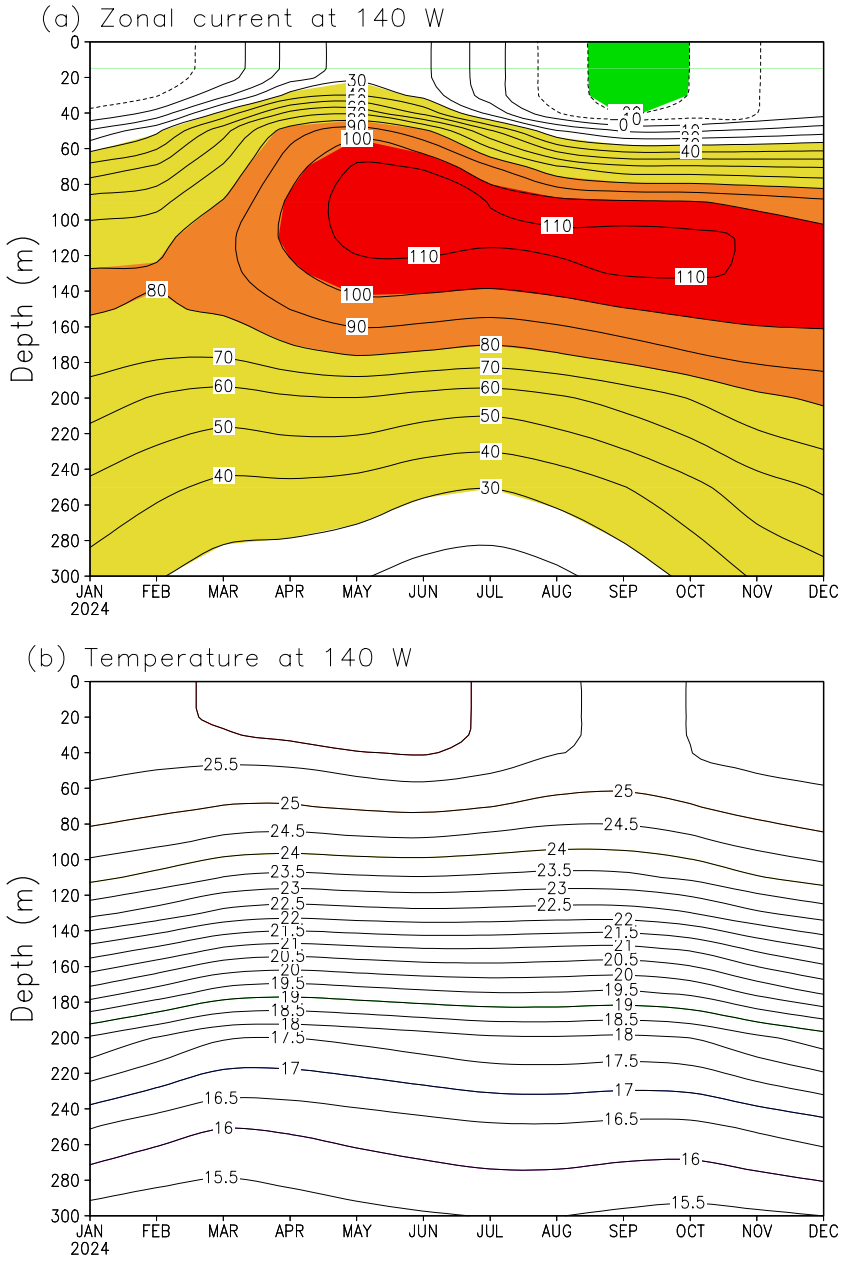

Fig. 10. Seasonal cycles of (a) zonal currents and (b) temperature fields at (140°W, 0°) simulated from the HCM. The contour interval is 10 cm s^{-1} in (a) and 0.5°C in (b).

cording to its classification as an HCM, such a model is economical in terms of computation, and yet can capture dominant SST–wind coupling over the Pacific basin, allowing interactions between processes in the tropics and subtropics to be adequately represented.

In addition, ENSO is affected by a variety of processes in the Pacific, including various forcings and feedbacks. For example, ENSO acts to produce perturbations in ocean biology, which can feed back to ENSO. As the simulated ENSO properties are sensitively dependent on the ways these processes are represented, their effects need to be adequately included in models. Based on our previous tropical modeling efforts, some important forcing and feedback processes affecting ENSO in the region can be adequately represented in the Pacific HCM, including SF, FWF, TIW, and OBH.

As expected, this simplified model tool is computationally efficient to run, and physically realistic enough to represent major components of the climate system over the Pacific basin. In particular, within this hybrid modeling context, forcing and feedback processes can be turned on or off, allowing their effects (individual or collective) on ENSO to be examined in a clean way. In addition, the related feedback intensities can be represented by parameters that are tunable, allowing their effects to be quantified. A variety of applications are anticipated for ENSO-related modeling studies. In this paper, very preliminary results from a reference run are

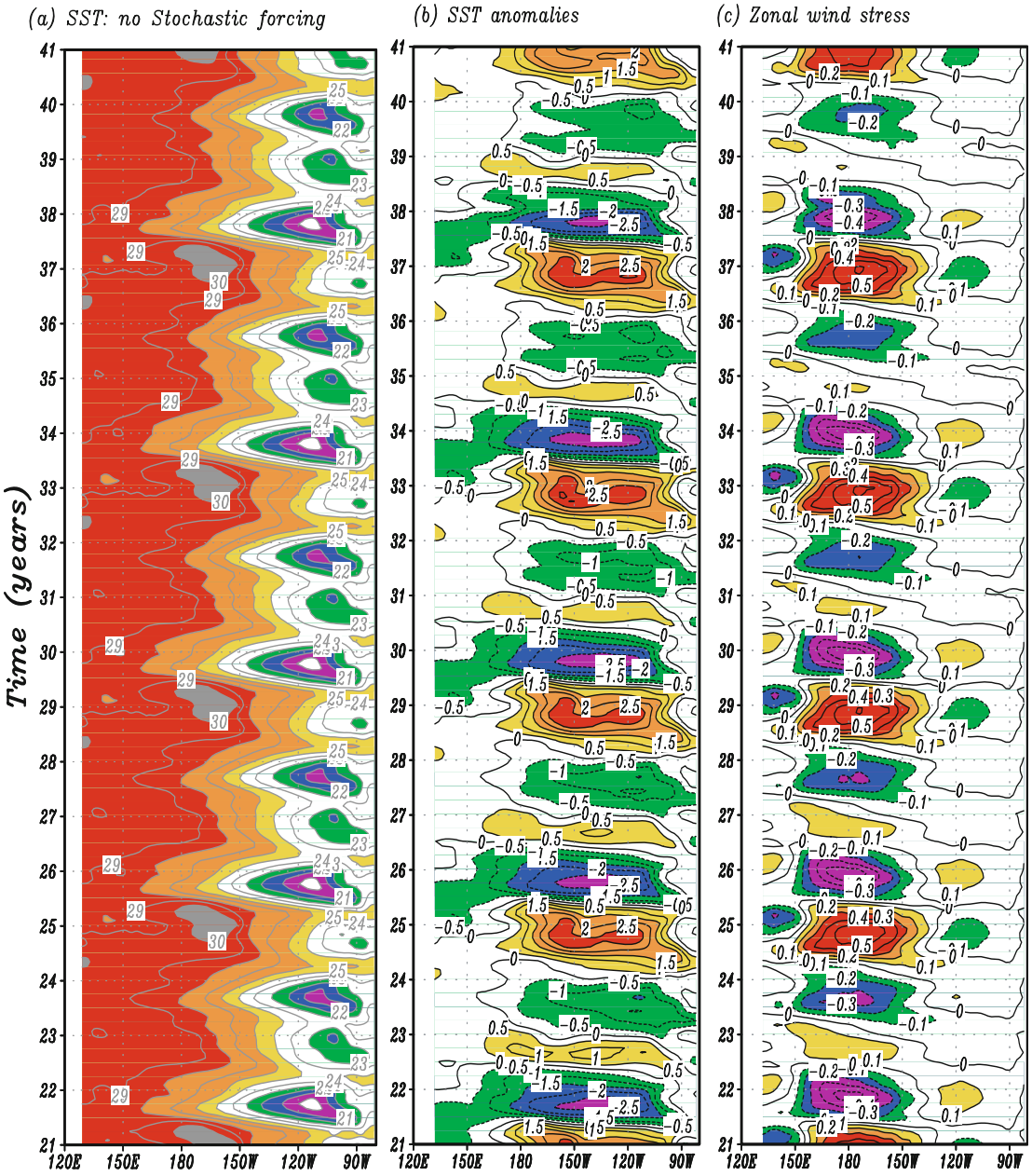

Fig. 11. Longitude–time sections along the equator for (a) SST, and interannual anomalies of (b) SST and (c) zonal wind stress simulated from the HCM. The contour interval is 1°C in (a), 0.5°C in (b), and 0.1 dyn cm^{-2} in (c).

used to demonstrate the HCM's performance, showing that it can reproduce quite well the mean ocean state, seasonal cycle and interannual variability associated with ENSO. For example, the Pacific-domain model depicts the well-defined mean water pathways from the subtropics to the tropics in the western Pacific through the LLWBC and NECC, and from the west to the east at the equator through the EUC pathways, respectively. As such, thermal conditions in the subtropical subduction regions can affect SST in the eastern equatorial Pacific.

In addition, a novel way of making use of satellite data is demonstrated in this paper. Note that some processes are still difficult to be adequately represented in current climate models. For example, ENSO can be modulated by ocean biology-induced heating, but this effect cannot be represented in physical models without a comprehensive marine ecosystem model. As satellite ocean color data are now available, and can capture interannual ocean biology variability associated with ENSO, they are used to parameterize these processes for climate modeling studies. As detailed in Zhang et al. (2011), the relationships between ocean biology fields (e.g., the penetration depth, H_p) and physical states (e. g., sea surface temperature) can be derived from satellite data, and be used to construct an empirical parameterization that is incorporated

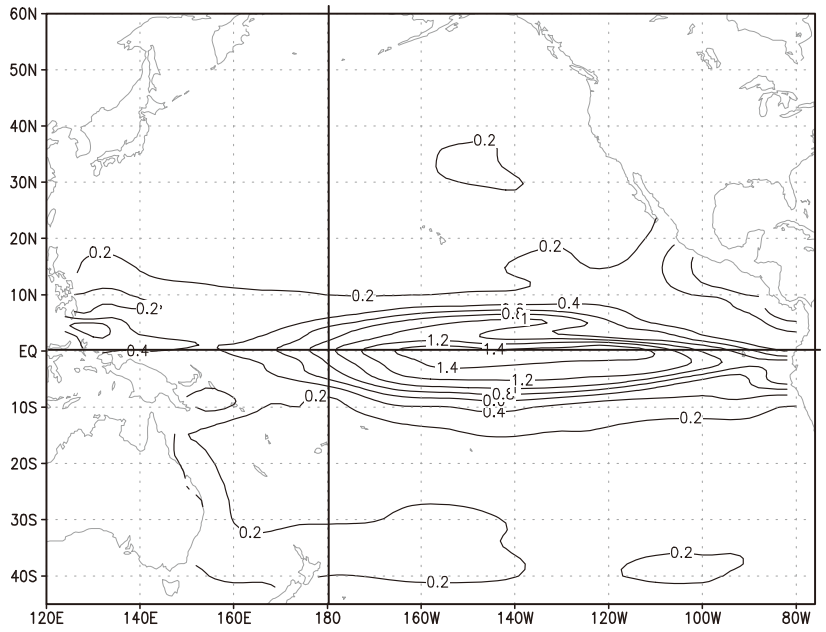

Fig. 12. Horizontal distribution of the standard deviation for interannual SST variability simulated from the reference run. The contour interval is 0.2°C.

in a climate model to represent ocean biology-induced heating effects. Also, TIWs are small-scale intraseasonal signals that are difficult to represent in large-scale climate models. However, high-resolution SST and surface wind data from satellites can be used to parameterize TIW wind feedback, which is included in the HCM. As such, vastly different processes at spatiotemporal scales can be integrated within a hybrid modeling context; multiscale interactions between TIW and ENSO can be examined. As demonstrated in this work, these approaches can be directly applied to any fully coupled model to adequately represent the related forcing and feedback processes.

The coupled ocean–atmosphere model developed for the entire Pacific in this work is classified as a hybrid model, which has disadvantages as other HCMs do (e.g., Zhu et al., 2011). For example, the HCM is designed to couple a basin-scale OGCM to a statistical atmospheric model, which provides the ocean with three forcing fields (wind stress, freshwater flux and heat flux). The forcings are constructed to consist of the climatological fields and, where appropriate, interannual anomaly fields; the former are prescribed from observed data and the latter are represented as functions of their corresponding interannual SST anomalies (which are also determined using statistical analysis methods from observed historical data). Thus, the model is designed, more or less, to "nudge" the ocean climate towards the observed one, and thus the HCM essentially represents an anomaly coupling between the atmosphere and ocean. As a result, the model simulations can be dependent on the ways the climatological fields are prescribed and/or statistical anomaly models are constructed (including time period and datasets used). In addition, interannual anomalies are represented as a feedback model without detailed processes in the atmosphere. In particular, the stochastic nature of atmospheric processes has not been taken into account adequately.

Some discrepancies are evident in the reference run. For example, the simulated ENSO events are far too regular, dominated by two-year oscillation. These discrepancies are partially related with the fact that some forcing and feedback processes are lacking in the reference HCM simulation. Further improvements are clearly needed and expected when these feedback processes are adequately included in the HCM. Indeed, preliminary testing indicates that stochastic forcing of wind can exert a significant influence on ENSO; when it is included in the HCM, the simulated ENSO events become irregular, yielding a more comparable result with observations. In Part II of this study, various factors affecting ENSO properties will be examined individually or collectively. The HCM with adequately represented forcing and feedback effects will be used to decipher relationships between forcing/feedback processes and ENSO modulations, multi-process interactions on various spatiotemporal scales, and interplay between processes involving the tropics and subtropics and midlatitudes, respectively.

Acknowledgements. The author would like to thank Drs. HU Dunxin and MU Mu for their comments. The author wishes to thank the two anonymous reviewers for their numerous comments that helped to improve the original manuscript. This research was supported by the CAS Strategic Priority Project (the Western Pacific Ocean System: Structure, Dynamics and Consequences, WPOS), a China 973 project (Grant No. 2012CB956000), the Institute of Oceanology, Chinese Academy of Sciences (IOCAS), and the National Natural Science Foundation of China (No. 41206017).

REFERENCES

Ballabrera-Poy, J., R. Murtugudde, R.-H. Zhang, and A. J. Busalacchi, 2007: Coupled ocean–atmosphere response to seasonal modulation of ocean color: Impact on interannual climate simulations in the tropical Pacific. *J. Climate*, **20**, 353–374.

Barnett, T. P., M. Latif, N. Graham, M. Flugel, S. Pazan, and W. White, 1993: ENSO and ENSO-related predictability. Part I: Prediction of equatorial Pacific sea surface temperature with a hybrid coupled ocean-atmosphere model. *J. Climate*, **6**, 1545–1566.

Bjerknes, J., 1969: Atmospheric teleconnections from the equatorial Pacific. *Mon. Wea. Rev.*, **97**, 163–172.

Bryden H. L., and E. C. Brady, 1989: Eddy momentum and heat fluxes and their effects on the circulation of the equatorial Pacific Ocean. *J. Mar. Res.*, **47**, 55–79.

Chang, P., L. Ji, and R. Saravanan, 2001: A hybrid coupled model study of tropical Atlantic variability. *J. Climate*, **14**, 361–390.

Chelton, D. B., S. K. Esbensen, M. G. Schlax, N. Thum, M. H. Freilich, F. J. Wentz, C. L. Gentemann, M. J. McPhaden, and P. S. Schopf, 2001: Observations of coupling between surface wind stress and sea surface temperature in the eastern tropical Pacific. *J. Climate*, **14**, 1479–1498.

Chen, D., L. M. Rothstein, and A. J. Busalacchi, 1994: A hybrid vertical mixing scheme and its application to tropical ocean models. *J. Phys. Oceanogr*., **24**, 2156–2179.

Fedorov, A. V., and S. G. H. Philander, 2000: Is El Niño changing? *Science*, **228**, 1997–2002.

Gent, P., and M. A. Cane, 1989: A reduced gravity, primitive equation model of the upper equatorial ocean. *J. Compute. Phys.*, **81**, 444–480.

Gu, D.-F., and S. G. H. Philander, 1997: Interdecadal climate fluctuations that depend on exchanges between the tropical and extratropics. *Science*, **275**, 805–807.

Jochum, M., R. Murtugudde, R. Ferrari, and P. Malanotte-Rizzoli, 2005: The impact of horizontal resolution on the equatorial mixed layer heat budget in ocean general circulation models. *J. Climate*, **18**, 841–851.

Kalnay, E., and Coauthors, 1996: The NMC/NCAR reanalysis project. *Bull. Amer. Meteor. Soc*., **77**, 437–471.

Kessler, W. S., L. M. Rothstein, and D. Chen, 1998: The annual cycle of SST in the eastern tropical Pacific, diagnosed in an ocean GCM. *J. Climate*, **11**, 777–799.

Kirtman, B. P., and P. S. Schopf, 1998: Decadal variability in ENSO predictability and prediction. *J. Climate*, **11**, 2804–2822.

Kleeman, R., J. P. McCreary, and B. A. Klinger, 1999: A mechanism for generating ENSO decadal variability. *Geophys. Res. Lett.*, **26**, 1743–1746.

Lewis, M. R., M. E. Carr, G. C. Feldman, W. Esias, C. McClain, 1990: Influence of penetrating solar radiation on the heat budget of the Equatorial Pacific. *Nature*, **347**, 543–546.

Levitus, S., J. I. Antonov, T. P. Boyer, 2005: Warming of the World Ocean, 1955–2003. *Geophys. Res. Lett.*, **32**, L02604, doi: 10.1029GL021592.

McClain, C. R., M. L. Cleave , G. C. Feldman, W. W. Gregg, S. B. Hooker , N. Kuring, 1998: Science quality SeaWiFS data for global biosphere research. *Sea Technol.*, **39**, 10–16.

McCreary, J. P., and P. Lu, 1994: Interaction between the subtropical and equatorial ocean circulations: The subtropical gyre. *J. Phys. Oceanogr.*, **24**, 466–497.

Monterey, G. I. Levitus, S., 1997: Seasonal variability of mixed layer depth for the World Ocean. NOAA NESDIS Atlas 14, Natl. Oceanic and Atmos. Admin., Silver Spring, Md., 100 pp.

Murtugudde, R., and A. J. Busalacchi, 1998: Salinity effects in a tropical ocean model. *J. Geophys. Res.*, **103**, 3283–3300.

Murtugudde, R., R. Seager, and A. J. Busalacchi, 1996: Simulation of tropical oceans with an ocean GCM coupled to an atmospheric mixed layer model. *J. Climate*, **9**, 1795–1815.

Murtugudde, R., J. Beauchamp, C. R. McClain, M. Lewis, and A. J. Busalacchi, 2002: Effects of penetrative radiation on the upper tropical ocean circulation. *J. Climate*, **15**, 470–486.

Reynolds, R. W., N. A. Rayner, T. M. Smith, D. C. Stokes, and W. Wang, 2002: An improved *in-situ* and satellite SST analysis for climate. *J. Climate*, **15**, 1609–1625.

Roeckner, E., and Coauthors, 1996: The atmospheric general circulation model ECHAM4: Model description and simulation of present day climate. Rep. 218, Max-Planck-Institut fur Meteorologie, 90 pp.

Rothstein, L. M., R.-H. Zhang, A. J. Busalacchi, and D. Chen, 1998: A numerical simulation of the mean water pathways in the subtropical and tropical Pacific Ocean. *J. Phys. Oceanogr.*, **28**, 322–343.

Seager, R., M. Blumenthal, and Y. Kushinir, 1995: An advective atmospheric mixed layer model for ocean modeling purposes: Global simulation of surface heat fluxes. *J. Climate*, **8**, 1951–1964.

Wang, B., and S.-I. An, 2001: Why the properties of El Nino changed during the late 1970s. *Geophys. Res. Lett.*, **28**, 3709–3712.

Wentz, F. J., C. Gentemann, D. Smith, and D. Chelton, 2000: Satellite measurements of sea surface temperature through clouds. *Science*, **288**, 847–850.

Xie, P., and P. Arkin, 1995: An intercomparison of gaobservations and satellite estimates of monthly precipitation. *J. Appl. Meteor.*, **34**, 1143–1160.

Zebiak, S. E., and M. A. Cane, 1987: A model El Niño/ Southern Oscillation. *Mon. Wea. Rev*., **115**, 2262–2278.

Zhang, R.-H., and S. Levitus, 1997: Interannual variability of the coupled tropical Pacific ocean–atmospheric system associated with the El Niño-Southern Oscillation. *J. Climate*, **10**, 1312–1330.

Zhang, R.-H., and L. M. Rothstein, 1998: On the phase propagation and relationship of interannual variability in the tropical Pacific climate system. *Climate Dyn.*, **14**, 713–723.

Zhang, R.-H., and S. E. Zebiak, 2002: Effect of penetrating momentum flux over the surface mixed layer in a z-coordinate OGCM of the tropical Pacific. *J. Phys. Oceanogr.*, **32**, 3616–3637.

Zhang, R.-H., and A. J. Busalacchi, 2005: Interdecadal changes in properties of El Niño in an intermediate coupled model, *J. Climate*, **18**, 1369–1380.

Zhang, R.-H., and A. J. Busalacchi, 2008: Rectified effects of tropical instability wave (TIW)-induced atmospheric wind feedback in the tropical Pacific. *Geophys. Res. Lett.*, **35**, L05608, doi: 10.1029/2007GL033028.

Zhang, R.-H., and A. J. Busalacchi, 2009a: Freshwater flux (FWF)-induced oceanic feedback in a hybrid coupled model of the tropical Pacific. *J. Climate*, **22**, 853–879.

Zhang, R.-H., and A. J. Busalacchi, 2009b: An empirical model for surface wind stress response to SST forcing induced by tropical Instability waves (TIWs) in the eastern equatorial Pa-

cific. *Mon. Wea. Rev.*, **137**, 2021–2046.

Zhang, R.-H., L. M. Rothstein, and A. J. Busalacchi, 1998: Origin of upper-ocean warming and El Niño change on decadal scale in the tropical Pacific Ocean. *Nature*, **391**, 879–883.

Zhang, R.-H., L. M. Rothstein, and A. J. Busalacchi, 1999: Interannual and decadal variability of the subsurface thermal structure in the Pacific Ocean: 1961–90. *Climate Dyn.*, **15**, 703–717.

Zhang, R.-H., T. Kagimoto, and S. E. Zebiak, 2001: Subduction of decadal North Pacific thermal anomalies in an ocean GCM, *Geophys. Res. Lett.*, **28**, 2449–2452.

Zhang, R.-H., S. E. Zebiak, R. Kleeman, and N. Keenlyside, 2003: A new intermediate coupled model for El Niño simulation and prediction. *Geophys. Res. Lett.*, **30**, 2012, doi: 10.1029/2003GL018010.

Zhang, R.-H., A. J. Busalacchi, and R. G. Murtugudde, 2006: Improving SST anomaly simulations in a layer ocean model with an embedded entrainment temperature submodel. *J. Climate*, **19**, 4638–4663.

Zhang, R.-H., A. J. Busalacchi, and D. G. DeWitt, 2008: The roles of atmospheric stochastic forcing (SF) and oceanic entrainment temperature (T_e) in decadal modulation of ENSO. *J. Climate*, **21**, 674–704.

Zhang, R.-H., A. J. Busalacchi, X. Wang, J. Ballabrera-Poy, R. G. Murtugudde, E. C. Hackert, and D. Chen, 2009: Role of ocean biology-induced climate feedback in the modulation of El Niño-Southern Oscillation. *Geophys. Res. Lett.*, **36**, L03608, doi: 10.1029/2008GL036568.

Zhang, R.-H., D. Chen, and G. Wang, 2011: Using satellite ocean color data to derive an empirical model for the penetration depth of solar radiation (H_p) in the tropical Pacific ocean. *J. Atmos. Oceanic Technol.*, **28**, 944–965.

Zhang, R.-H., F. Zheng, J. Zhu, Y. Pei, Q. Zheng, and Z. Wang, 2012: Modulation of El Niño-Southern Oscillation by freshwater flux and salinity variability in the Tropical Pacific. *Adv. Atmos. Sci.*, **29**, 647–660, doi: 10.1007/s00376-012-1235-4.